LU-TP 21-26
June 2021

Multiplicity and Classification of Final State Particles in Herwig7

Carl Rosenkvist

Department of Astronomy and Theoretical Physics, Lund University

Bachelor thesis supervised by Patrick Kirchgaeßer and Leif Lönnblad

LUND UNIVERSITY

Abstract

In this work we investigate the hard and soft interactions in the multiple parton interactions (MPI) simulation in `Herwig7`. The investigation covers how the number of soft and hard interactions in an event is linked to the multiplicity of final state particles. We also present a labeling system for particles produced by different interactions, which we then use to classify the final state particles. We also demonstrate how this labeling system can be used as a tool to disentangle different contributions to a given observable. The observables we investigated are the charged multiplicity and the charged transverse momentum. We observed a large contribution from diffractive events in the high multiplicity region and therefore we produced the invariant mass distribution of primary clusters. From this distribution, we observed that primary clusters from diffractive events have a long tail towards high invariant mass.

Popular Science Summary

Some particle physicists' job is similar to that of a detective as both use clues to recreate events. The particle physicist's event is the interactions of particles in the particle collider, and the clues are called observables which are physical quantities measured by the detector. The reason for this similarity is that elementary particles like quarks carry color charge but are forced by nature to exist in constellations that are colorless. This restriction is called color-confinement and is the reason why the interaction of two quarks can not be observed directly. This means that particle collisions can be thought to happen inside a box which we cant see into. Theoretical models must thus explain the interactions and through simulating events through event generation these models can be compared to real data.

Collisions of composite particles, like e.g protons, are described by their collisions of their constituents called partons. The interactions of partons are the beginnings of the complex processes which eventually result in observable particles in detectors. Due to the proton's composite nature, there is a possibility for several partons to interact in the same proton collision. These additional interactions make it harder to understand which interaction observable particles originate from.

To understand how the different interactions contribute to observable particles we use the event generator `Herwig7`. We use this event generator to investigate the link between the number of interactions and the number of observable particles. Furthermore we introduce a labeling system which allows us to track particles produced from different interactions. The difference in real data and simulation can be investigated by the labeling system such that we can pinpoint which interaction might be responsible. Therefore the labeling system is a useful tool for model investigation and event generator improvements.

Contents

1 Introduction

Many high energy collider experiments like the large hadron collider at CERN involve hadron collisions, which are described by the parton model. In this model each hadron is described as a bunch of partons which may interact when the hadrons pass each other. The interactions of constituents belonging to different hadrons are the beginnings of the complex processes which eventually result in the observable hadrons in detectors. The high transverse momentum scattering between two colliding partons, also called hard scattering, results in the pair leaving the hadron and becoming jets. Aside from the hard scattering and the resulting jets we also have the underlying event which is the rest of the hadronic activity.
One way to describe the underlying event is through the fact that hadrons are composite objects, thereby it is possible for multiple partons to interact in the same hadron-hadron collision. These additional interactions are termed multiple parton interactions (MPI) and they contribute to background activity in hadron colliders. Furthermore, after the hard scattering, the remnant of the hadron, the so-called beam remnant will also contribute to the underlying event.
MPI is currently used to explain otherwise unexplainable phenomena such as: the cross sections of multi-jet production, the survival probability of large rapidity gaps and more [1]. Additionally, MPI models are used in event generators such as `Herwig7` and `Pythia` [2, 3]. The comparison of simulated final state multiplicity distributions to data shows that there is a need for a MPI to accurately simulate data. This argument is presented in [4] with a comparison between an ATLAS measurement of the charged-track multiplicity at 7 TeV to simulations with and without MPI switched on. The predicted multiplicity distribution from a MPI model agrees with the experimental data, and is therefore a strong argument for these models. Furthermore, MPI are also important for the modeling of low transverse momentum interactions, so-called soft interactions.
In this work, we use the event generator `Herwig7` which uses MPI to simulate the underlying event. The additional interactions between partons are simulated as semi-hard interactions which are described by perturbation theory. Soft interactions between beam remnants are also included, but they can not be described by perturbation theory since it breaks down for low transverse momentum interactions. Instead, non-perturbative models are used for the simulation of soft MPI.
The particles created in an MPI simulation will contribute to final state multiplicity and thus in principle all kinds of observables. How much these particles contribute to observables and final state multiplicity is currently not known in `Herwig7`. Therefore, in this work we investigate how the number of MPI affects the final state multiplicity. Furthermore we introduce a labeling system such that the contributions of different interactions to the final state can be disentangled. We also demonstrate how this labeling system can be used as a tool to observe different contributions to a given observable.
In section 2 we present a brief overview of the event generation with `Herwig7` and the simulation of MPI. This section is followed by section 3 in which we motivate the analysis and

then describe it in section 4. In section 5 the results are presented and discussed. Then, in section 6 we draw conclusions from the results and in section 7 we give an outlook.

2 Background Theory

In this section we present the necessary theory to follow the analysis method in section 4 and the motivation for the labeling system in section 3. For this purpose the overview includes a description of event generation with `Herwig7` and MPI.

2.1 Event generation with Herwig7

The overview of event generation in this work is based on [3–5], these papers are recommended for further and more detailed reading.
The simulation of hadron collision usually begins with the hard subprocess which is the high energy collision of two constituents belonging to different colliding hadrons. The distributions of energy and relative angles is obtained from a Feynman diagram description of the physical subprocess. Using Feynman diagrams for the computation of matrix elements is made possible due to the fact that the energy scale of the subprocess is sufficient for perturbation theory.
The hard subprocess is calculated with fixed order matrix elements due to computational limits. However, any fixed order is insufficient for a full picture of the process, including internal structure of jets and the distributions of accompanying particles. The effect of higher orders can be simulated by using a parton shower algorithm. This algorithm is formulated as an evolution in momentum transfer from the high scales of the hard subprocess down to the low scales of hadron confinement. The physics behind parton showers is that the colored particles produced from the hard scattering will produce QCD radiation which in turn can produce more particles and more radiation.
In the large number of colors limit, the ingoing and outgoing particles from an interaction are color connected [6]. A color connection between two particles means that one of them is carrying the anti-color to the other's color. These color connections are then used to resolve the color charges at the confinement scale in the process of producing hadrons which is called hadronization. Different hadronization models exist, and `Herwig7` uses the cluster model [3]. This model is based on the color pre-confinement property of angular-ordered showers [7], which allows for the formation of color singlets out of two color connected particles. These color singlets are termed clusters and they are described as excited pre-hadronic states. To form these clusters all gluons at the confinement scale are non-perturbativly split into quarks.
In reality where there are only three colors there is ambiguity for which color-singlet partons belong to. Additionally due to the large density of color charges in an accelerator, the partons may interact in ways which event generators do not account for. However, by

using color reconnection models to reassign parton color, these uncertainty effects can be somewhat accounted for [8]. Color reconnection in `Herwig7`, is used to rearrange cluster constituents, which results in a different input for the hadronization model. The implementation of color reconnection in `Herwig7` is done by evaluating other color connections to minimize the invariant mass of clusters [5]. A possible outcome of color recconection is shown in figure 1

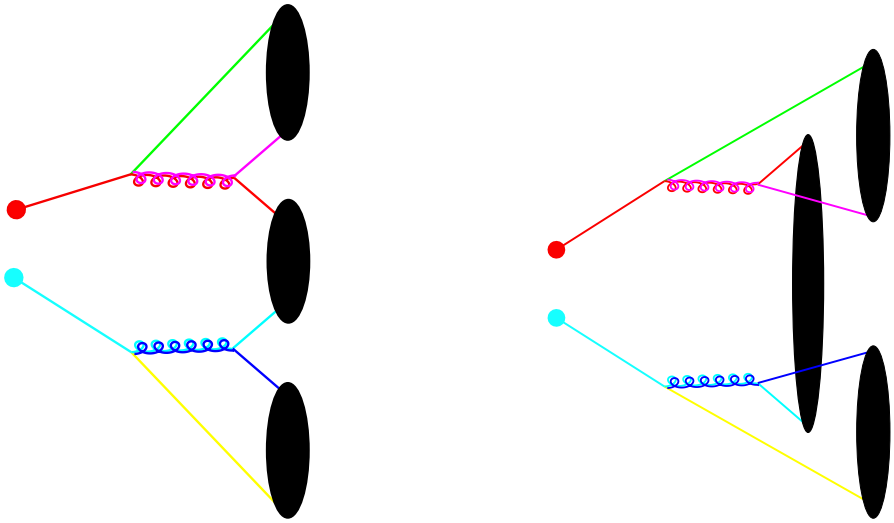

(a) (b)

Figure 1: (a): From the left, two incoming quarks which are color connected. At the right clusters are formed of color connected quarks. (b): Same particles as in (a) but with alternative cluster formation due to color reconnection. The colors in both figures represent color charge.

Additionally, depending on it's invariant mass, a cluster can split into two new clusters through cluster fission. The final clusters will decay into hadrons which will further decay if unstable. This is the end of the event generation and the hadrons at this stage are the final state particles.
However this is not the full picture, the underlying event is also simulated and connected to the rest of the event generation, including parton shower and hadronization. The underlying event consists of the additional hard scatterings and the particles left behind from the main hard subprocess, the beam remnants. In `Herwig7` the additional hard scatterings are simulated as $2 \to 2$ QCD processes and the interactions of beam remnants are non-perturbative. Furthermore, diffractive events are also included in the simulation. These events are characterized as proton collision without quantum number exchange, and therefore with little hadronic activity. More intuitively diffractive scattering can be thought of as inelastic scattering with no hard interactions between partons, but where the proton still breaks up. In `Herwig7`, diffractive events are simulated without MPI.

2.2 Multiple Parton Interactions

To start to think about MPI simulation we begin with the fact that $2 \to 2$ QCD interactions are dominated by t-channel gluon exchange [2], thereby the differential cross section diverges for $p_\perp \to 0$ as

$$\frac{\mathrm{d}\sigma}{\mathrm{d}p_\perp^2} \sim 1/p_\perp^4. \tag{2.2.1}$$

The total hard-scattering cross section above some $p_\perp^{\min}$ is given by

$$\sigma_{\mathrm{hard}}(p_\perp^{\min}) = \int_{(p_\perp^{\min})^2}^{s/4} \frac{\mathrm{d}\sigma}{\mathrm{d}p_\perp^2} \mathrm{d}p_\perp^2. \tag{2.2.2}$$

The total hard cross section is thereby also divergent for $p_\perp^{\min} \to 0$. This divergence may result in σ_{hard} being larger than the total inelastic non-diffractive cross section, σ_{nd}. However this is not a contradiction, since σ_{hard} does not give the hadronic cross section but the partonic one. Since protons are composite objects, we may think of them as bunches of partons, which may interact when hadrons pass through each other. By this logic, the ratio $\sigma_{\mathrm{hard}}(p_\perp^{\min})/\sigma_{\mathrm{nd}}$ would then be the average number of partonic interactions above $p_\perp^{\min}$ in an event, which may be larger than unity. Below the $p_\perp^{\min}$ threshold, perturbative QCD breaks down and thus non-perturbative models need to take over.

2.3 Eikonal MPI Model for Underlying Event Simulation

The first detailed model of MPI physics was introduced in [9] which is used as a basis for MPI models in event generators such as `Herwig7` and `Pythia`. In the case of `Herwig7`, an eikonal MPI model is used. The overview of the eikonal model in sections 2.3.1 and 2.3.2 is based on [3, 10]. The term eikonal comes from the eikonal approximation which is valid in the high energy limit for non-relativistic scattering. In this approximation the elastic scattering amplitude can be written in terms of a function which only depends on the impact parameter and collision energy. The impact parameter is defined as the perpendicular distance between the projectile path and the center of a potential field produced by the target.

2.3.1 Hard Interactions

The eikonal model used by `Herwig7` is based on the assumption that at a fixed impact parameter, b, individual scatterings are independent and the distributions of partons factorizes with respect to b and s. Thereby the number of scatterings can be written as

$$\langle n(\mathbf{b}, s) \rangle = A(b)\sigma_{\mathrm{hard}}^{\mathrm{inc}}(s; p_\perp^{\min}) \tag{2.3.3}$$

Where $A(b)$ is a function describing the overlap of the colliding hadrons and $\sigma_{\text{hard}}^{\text{inc}}$ is the cross section for the production of a pair of partons with $p_\perp > p_\perp^{\min}$. The overlap function's dependence on the impact parameter is shown in figure 2.

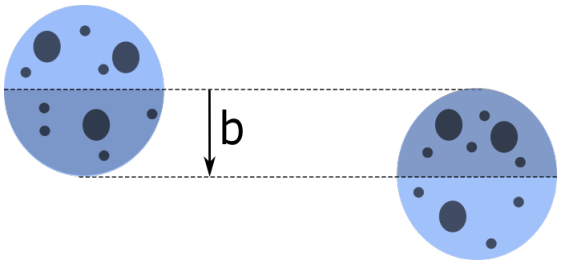

Figure 2: A schematic view of how the overlap function in a proton collision depends on the impact parameter. The overlap is the darker area of the protons. The larger dark circles represent the valence quarks while the smaller are gluons or sea quarks.

The impact overlap function is modeled after the spatial distribution of electric charge inside the nucleus

$$A(b;\mu) = \frac{\mu^2}{96\pi}(\mu b)^3 K_3(\mu b) \tag{2.3.4}$$

where μ is the inverse proton radius and $K_3(x)$ is the modified Bessel function of the third kind. Since the spatial parton distribution is not assumed to be exactly like the electric charge distribution, μ is treated as a free parameter of the model. From the assumption that different scatters are uncorrelated for a fixed impact parameter follows a Poissonian distribution for the number of scatters, n

$$\mathcal{P}_n(b,s) = \frac{\langle n(\mathbf{b},s)\rangle^n}{n!} e^{-\langle n(\mathbf{b},s)\rangle}. \tag{2.3.5}$$

This distribution is then used to write the unitarized cross section

$$\sigma_{\text{inel}}(s) = \int \mathrm{d}^2\mathbf{b} \sum_{k=1}^{\infty} \mathcal{P}_k(b,s) = \int \mathrm{d}^2\mathbf{b}\left[1 - e^{-\langle n(\mathbf{b},s)\rangle}\right]. \tag{2.3.6}$$

For the Monte Carlo implementation the probability of having n scatterings given that there is at least one

$$P_n(s) = \frac{\int \mathrm{d}^2\mathbf{b}\mathcal{P}_n(b,s)}{\int \mathrm{d}^2\mathbf{b} \sum_{k=1}^{\infty} \mathcal{P}_k(b,s)}. \tag{2.3.7}$$

Equation 2.3.7 serves as the basis for multiple parton scattering events where the additional scatterings are simulated as semi-hard scatterings, i.e. QCD $2 \to 2$.

2.3.2 Soft Interactions

The eikonal model in Herwig7 is extended below $p_\perp^{\min}$, by using that the elastic scattering amplitude $a(\mathbf{b}, s)$ in impact parameter space can be written as

$$a(\mathbf{b}, s) = \frac{1}{2i}\big[e^{-\chi(\mathbf{b},s)} - 1\big], \tag{2.3.8}$$

where $\chi(\mathbf{b}, s)$ is a real eikonal function. The elastic scattering amplitude $\mathcal{A}(s, t)$ can be expressed as the Fourier transform of $a(\mathbf{b}, s)$. The optical theorem states that the total hadronic cross section is proportional to the elastic scattering amplitude at zero scattering angle [11]. Thereby, through the optical theorem we get the total pp cross section and the elastic cross section

$$\sigma_{\text{tot}}(s) = 2\int \mathrm{d}^2\mathbf{b}\big[1 - e^{-\chi(\mathbf{b},s)}\big], \quad \sigma_{\text{el}} = \int \mathrm{d}^2\mathbf{b}\big[1 - e^{-\chi(\mathbf{b},s)}\big]^2. \tag{2.3.9}$$

Then the inelastic cross section is the difference between the total and the elastic cross section, thus

$$\sigma_{\text{inel}} = \int \mathrm{d}^2\mathbf{b}\big[1 - e^{-2\chi(\mathbf{b},s)}\big]. \tag{2.3.10}$$

To regain equation 2.3.6, the eikonal function is chosen to be

$$\chi(\mathbf{b}, s) = \frac{1}{2}\langle n(\mathbf{b}, s)\rangle. \tag{2.3.11}$$

For the purpose of introducing additional scatters below the $p_\perp^{\min}$, equation 2.3.11 is identified to be the hard part of a universal eikonal function such that

$$\chi_{\text{tot}}(\mathbf{b}, s) = \chi_{\text{hard}}(\mathbf{b}, s) + \chi_{\text{soft}}(\mathbf{b}, s). \tag{2.3.12}$$

By imposing the assumptions that just like hard scatters the soft scatters are uncorrelated and also that probability distributions of semi-hard and soft scatters are independent, gives

$$\mathcal{P}_{h,n}(\mathbf{b}, s) = \frac{\big(\chi_{\text{hard}}(\mathbf{b}, s)\big)^h}{h!}\frac{\big(\chi_{\text{soft}}(\mathbf{b}, s)\big)^n}{n!}e^{-2\chi_{\text{tot}}(\mathbf{b},s)}. \tag{2.3.13}$$

Following the same steps as for equation 2.3.7 results in the probability of having exactly h semi-hard and n soft scatters in an inelastic event

$$P_{h,n}(s) = \frac{\int \mathrm{d}^2\mathbf{b}\,\mathcal{P}_{h,n}(\mathbf{b}, s)}{\int \mathrm{d}^2\mathbf{b}[1 - e^{2\chi_{\text{tot}}(\mathbf{b},s)}]}, \quad h + n \geq 1. \tag{2.3.14}$$

Equation 2.3.14 is used to create a matrix at the beginning of the simulation with its elements being a pair of the number of soft scatters and hard scatters and their corresponding probability. This matrix is then used to determine the number of hard and soft scatters in each event. The soft interactions in Herwig7 are modeled such that they produce a gluon ladder, where the gluons are distributed uniformly in rapidity.

3 Color Connections and Cluster Topologies

MPI in the underlying event will contribute with outgoing particles, and are therefore linked to the cluster formation. In the following we show typical QCD $2 \to 2$ interactions and the possible ruling color topologies to illustrate this link. The main hard interaction is simulated as $2 \to 2$ QCD processes, an example is $qq \to qq$ as shown in the figure 3.

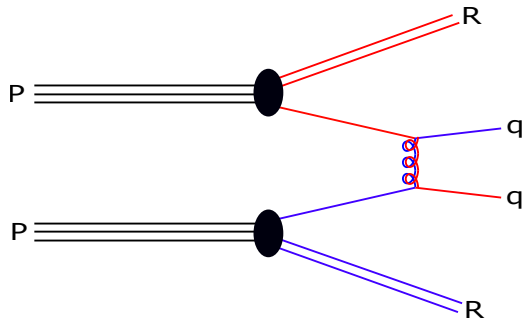

Figure 3: Color connections for a hard $qq \to qq$ process. The colored lines represent the color connections. P stands for proton, R is a remnant and q is a quark

From the color lines we can observe that the outgoing quarks are color connected to a remnant. Figure 3 is just one example. We could also have a $\bar{q}q \to q\bar{q}$ process as shown in the figure below

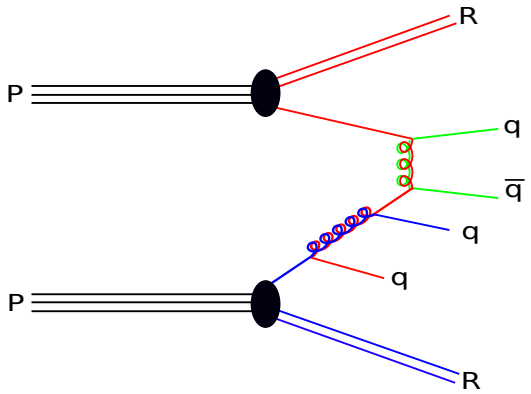

Figure 4: Color connections for a hard $\bar{q}q \to \bar{q}q$ process. The colored lines represent the color connections. P stands for proton, R is a remnant, q is a quark and $\bar{q}$ is an antiquark

Figure 4 also shows the forced splitting due to the model requirement that the main hard interaction needs to be evolved backwards to a valence quark [10]. The reason is that the cluster model requires an even input of particles to form the clusters. The forced splittings refers to the process by which the event generator ensures that in this case partons from the main hard interaction originate from a valence quark by either splitting gluons or quarks

from the hadron. The term backwards evolution just refers to that the event generator starts to simulate the interaction and then makes sure that it can be connected to the hadron.
Figure 3 and 4 are simple examples of the main hard subprocess. However in this work we are interested in the simulation of minimum bias events. The term minimum bias events refers to events selected in detectors with as little bias as possible from the event selection. These events in `Herwig7` are simulated without a main hard interaction, but instead with a dummy matrix element to split up the protons [3]. This matrix element is constructed such that it will have as little effect possible. Therefore the interaction is modeled with the exchange of a particle with the quantum numbers of the vacuum, the-so called pomeron [3]. The result of this matrix element is that the extracted quarks from the protons obtain no transversal momentum and no color is exchanged. The figure below shows the color connections due to the dummy matrix element.

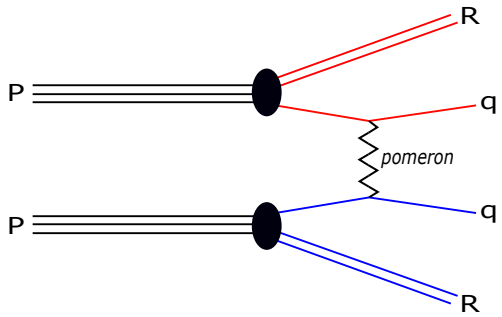

Figure 5: Color connections for a dummy process. The colored lines represent the color connections. P stands for proton, R is a remnant and q is a quark

The dummy process breaks up the proton and can be accompanied by MPI. The gluon ladder associated with the soft interaction carries no color connections to the remnants, thus it's effect on cluster topologies is straightforward. The gluons in the ladder are color connected to each other and thus will form clusters made by particles originating from the soft interaction. Therefore, particles originating from the soft interaction we refer to as soft particles. After the extraction of a valence parton the valence structure of the proton is exhausted, therefore semi-hard interactions are backwards evolved to a gluon from the hadron [3]. The figure below shows a $gg \to gg$ interaction.

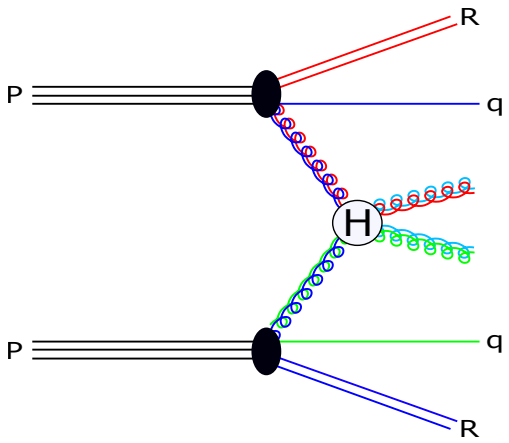

Figure 6: Color connections for a hard $gg \to gg$ process. The colored lines represent the color connections. P stands for proton, R is a remnant and q is a quark. The H denotes the hard interaction.

The quarks next to the remnants in figure 6 are the quarks extracted by the dummy process, which we also label as soft particles. We motivate the outgoing quarks from the dummy process as soft due to them having no transverse momentum. We refer to particles originating from the semi-hard interaction as hard particles. By observing the color connections in the figure we can expect clusters made from soft particles and hard particles. Furthermore we can also expect clusters formed by a remnant and a soft particle, a hard particle and a remnant. The $qq \to qq$ process which also leads to the production of additional quarks from the backwards evolution is shown below.

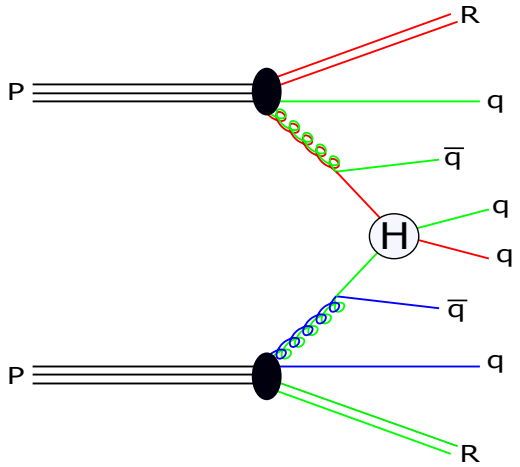

Figure 7: Color connections for a hard $qq \to qq$ process. The colored lines represent the color connections. P stands for proton, R is a remnant, q is a quark and $\bar{q}$ is an antiquark. The H denotes the hard interaction.

Due to the backwards evolution we have extra quarks which are also color connected to

other particles. The origin of these quarks is perturbative and since they can be described as additional hard radiation associated with the hard interaction, we choose to label them as hard. Through the origin based labels for particles we can classify the clusters by their constituents' origin as shown in figure 8.

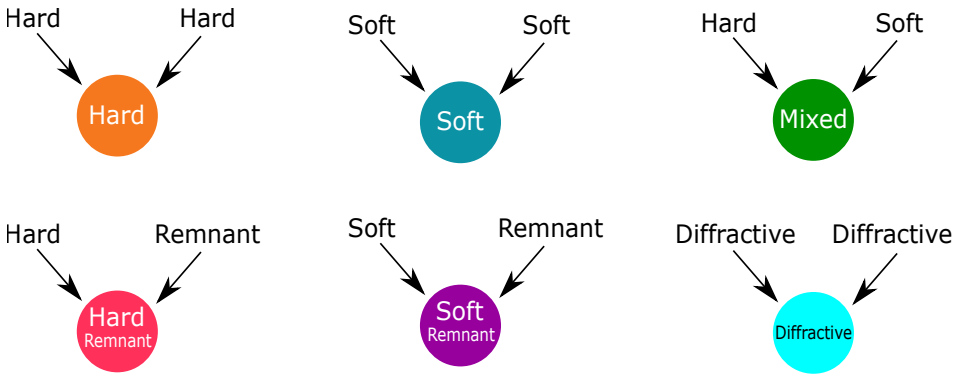

Figure 8: Scheme of the classification of clusters.

Since diffractive events are simulated without MPI, we label particles from events with zero MPI as diffractive. Furthermore, since color reconnection rearranges cluster constituents, we expect it to have an effect on the cluster topology.

4 Analysis

In this work we are using `Herwig` 7.2.2 and `ThePEG` 2.2.2, where the matrix associated with equation 2.3.14 is calculated at the beginning of the simulation. The matrix elements can be accessed when the matrix is referenced per event. The number of soft and hard interactions does however not tell us which particles in the simulation are hard or soft, but some results can already be drawn. We show the results of this part of the analysis in figure 9 in section 5.1.
In this work we introduce a label for the particles from the gluon ladder associated with the soft interaction. We do not label the beam-remnants soft, instead a unique label is used for remnants. With all the labels, we classify the clusters according to what the parents label were, e.g cluster with both parents labeled soft is classified as a soft cluster. For those not acquainted with the parent-child terminology, it is just what it sounds like: parents are ingoing particles to an interaction and children are outgoing particles from said interaction. We want to classify final state particles by what type of cluster it came from. For this purpose we use a search algorithm to look through the final state particle parents until it finds a cluster with no cluster parents, called a primary cluster. Then by using the labeling system we classify the final state particle either as hard, soft, mixed, hard-remnant or soft-remnant. Mixed is for particles coming from a primary cluster with a soft parent and a hard parent. Furthermore, we also chose to classify the final states particles from

events with 0 hard interactions and 0 soft interactions as diffractive. This includes events which are calculated according to the diffraction matrix element and also events with the dummy process but no additional hard and soft interactions.

5 Results and Discussion

Here we present and discuss the results obtained from the analysis of multiplicity with respect to the number of soft and hard interactions in section 5.1. Then in section 5.2 we present observables and investigate the different processes that contribute to them according to our labeling system. The cuts on the final state particles are $p_\perp > 100\,\mathrm{MeV}$ and $|\eta| < 2.5$.

5.1 Charged Final State Multiplicity

In figure 9a we show a heat map graph representing the average multiplicity with respect to the combinations of simulated soft and hard interactions. We observe that the graph implies that the final state multiplicity is not solely driven by the hard interactions but also depends on the number of soft interactions. This link between the final state multiplicity and MPI is expected, since more interactions in an event intuitively implies more final state particles. In figure 9b we show that the high multiplicity area is suppressed and the most common is to have an event with zero hard and zero soft interactions with low final state multiplicity.

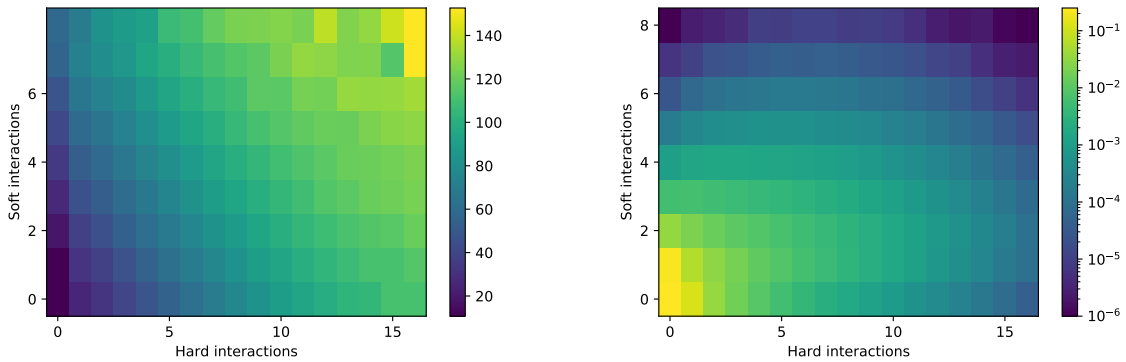

(a) (b)

Figure 9: (a) A heat map graph showing the average multiplicity of final states for combinations of hard and soft interactions. (b) A two-dimensional histogram of the number of hard and soft interactions in an event with a logarithmic scale.

In figure 10, we show with a bar graph and a scatter plot the average fraction of final states particles in an event for a given charged multiplicity originating from different clusters for a given charged multiplicity. We can observe a large contribution from hard clusters and mixed clusters at higher multiplicities. Furthermore the final states from mixed and hard remnant-clusters is more or less constant through the multiplicity range.

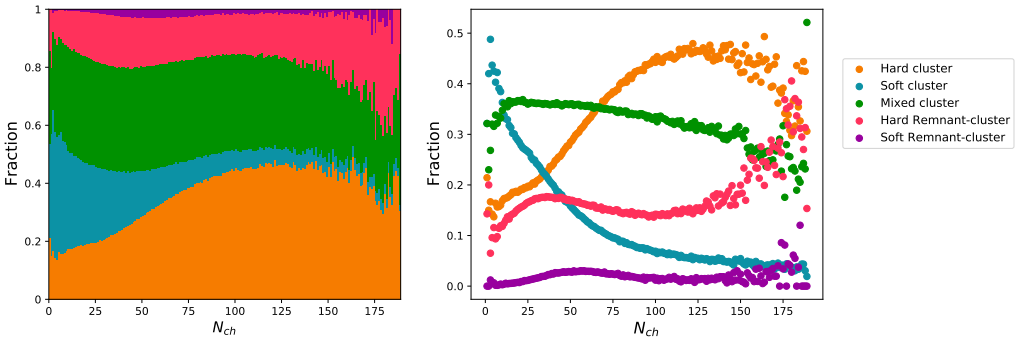

Figure 10: Average fraction of final states in an event from different clusters with color reconnection enabled represented by both a bar graph and a scatter plot. No diffractive events are included

From figure 10, we confirm that the high final state multiplicity comes from a combination of hard and soft interactions. However, the contribution from the soft interactions comes in the form of mixed clusters. The contribution from soft remnant-clusters was quite low as expected, since the dummy interaction only happens once per event and produces two soft quarks with zero $p_\perp$ color connected each to a remnant. In figure 11 we show the same graph of the fractions of different final states as in figure 10 but with color-reconnection disabled. From this figure we conclude that the mixed clusters and the hard remnant-clusters mainly come from the rearrangement of clusters due to color reconnection.

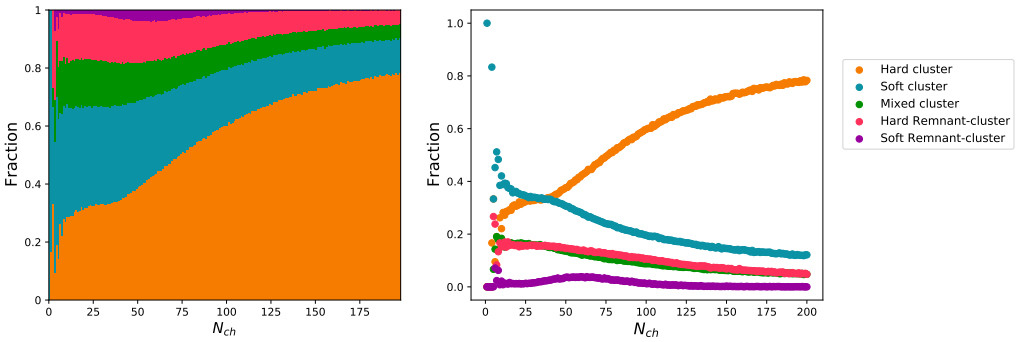

Figure 11: Average fraction of final state particles in an event from different clusters with color reconnection disabled represented by both a bar graph and a scatter plot. No diffractive events included

The soft-remnant particles are still present even without color reconnection which is expected since the dummy process produces soft particles which are color-connected to the remnants. Without color reconnection we observe that the high multiplicity region is dominated by contributions from hard clusters. Then, by comparing the results with and without color reconnection we conclude that we get a more diverse contribution in the higher multiplicity region with color reconnection.

5.2 Observable Composition

In figure 12 we present the decomposition of the charged multiplicity distribution compared to data from ATLAS.

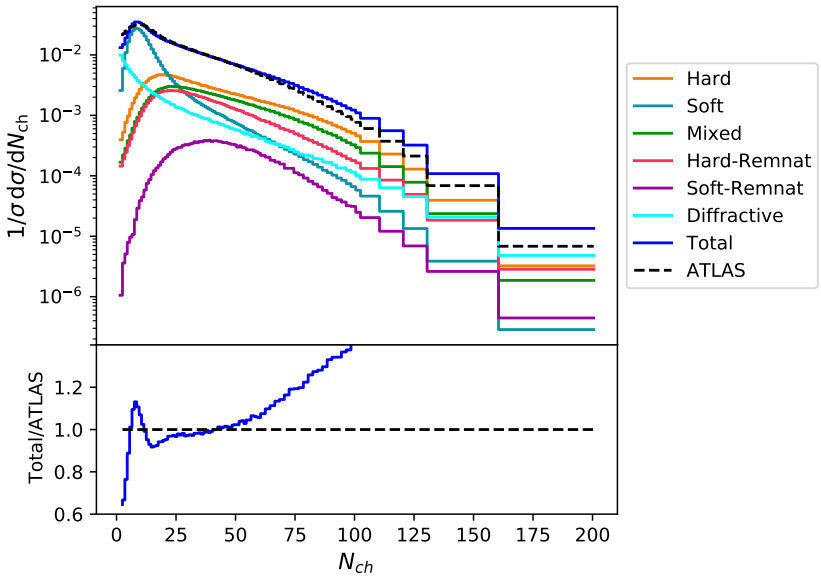

Figure 12: Charged multiplicity distribution at $\sqrt{s} = 7\,\text{TeV}$, track $p_\perp > 100\,\text{MeV}$ and $|\eta| < 2.5$, decomposed with the labeling system. Data from ATLAS [12].

We observe a peak structure due to soft final state particles roughly in the region $2 < N_{\text{ch}} < 20$. This peak deviates from the other contributions which are flatter in that region. The soft-remnant particles do not have this peak and thus this implies that the peak is unique to just soft final state particles explicitly from the gluon ladder. Furthermore, the large contribution from diffractive final state particles in the high multiplicity region is unexpected since diffractive events on average produce few final state particles. This observation therefore suggests that the distribution of diffractive final state particles has a long tail towards high multiplicity. We suspect that the reason is that primary clusters from diffractive events have a long tail toward high invariant mass, as seen in figure 15. Since a high invariant mass allows clusters to undergo cluster fission implies that this long tail can be the cause for the large diffractive contribution to charged multiplicity. Since

events with 0 hard and 0 soft interactions are also included in the diffractive label they contribute as well.
In figure 13 we show the charged particle $p_\perp$ distribution together with data from ATLAS. As expected the hard particles contribute the most for higher $p_\perp$, while the soft do not. We note that the deviation from the data in the large $p_\perp$ region is due to the decrease of the hard contribution. This drop in the hard contribution suggests too low production of particles from the hard interaction could be the cause. Furthermore the hard particles which are produced seem to get dragged down by a soft partner through color (re)connections.

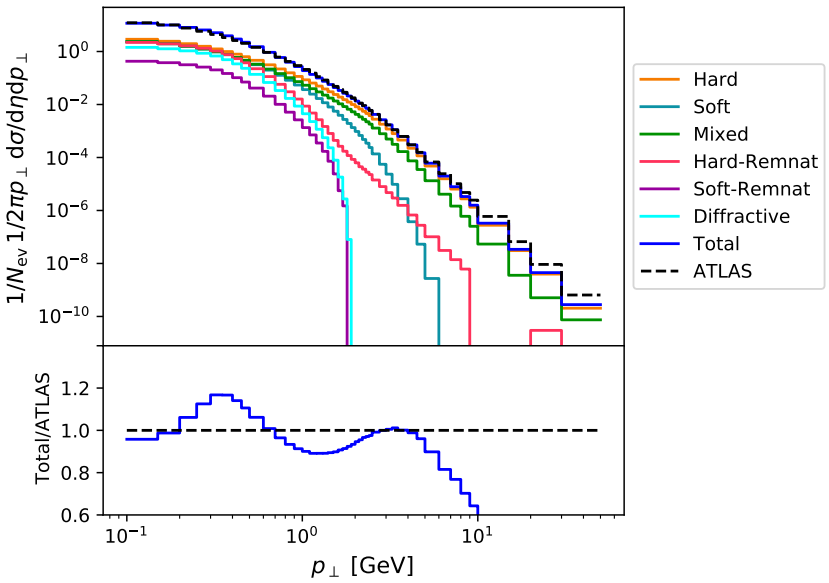

Figure 13: Charged particle distribution $p_\perp$ at $\sqrt{s} = 7\,\text{TeV}$, track $p_\perp > 100\,\text{MeV}$ and $|\eta| < 2.5$, for $N_{\text{ch}} \geq 2$. Data from ATLAS [12].

In figure 14 we show the $p_\perp$ distribution of the final state particles, but with a different normalization and scale than in figure 13. We observe in figure 14 that a suppressed fraction of the soft final state particles manage to have transverse momentum larger than $p_\perp^{\text{min}} = 2.87\,\text{GeV}$.

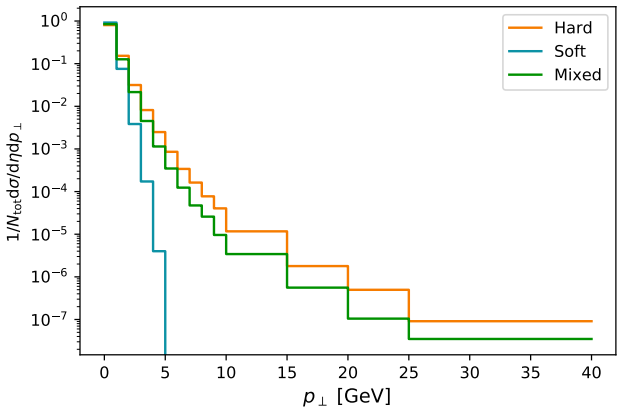

Figure 14: The $p_\perp$ distribution for hard, soft and mixed final state particles normalized to the total number of charged final state particles. $|\eta| < 2.5$ and $p_\perp > 100\,\text{MeV}$.

The fraction of the soft final state particles that have transverse momentum larger than $p_\perp^{\text{min}}$, although suppressed, is somewhat unexpected. The soft particles come from interactions below $p_\perp^{\text{min}}$ and should thus stay below this threshold. However since this is not the case, we expect that the particles or/and the clusters obtain additional transverse momentum. A plausible explanation comes from the fact that when clusters fission they obtain additional transverse momentum [3].

5.3 Invariant Mass Distribution of Primary Clusters

In figure 15 we present the invariant mass distribution of primary clusters.

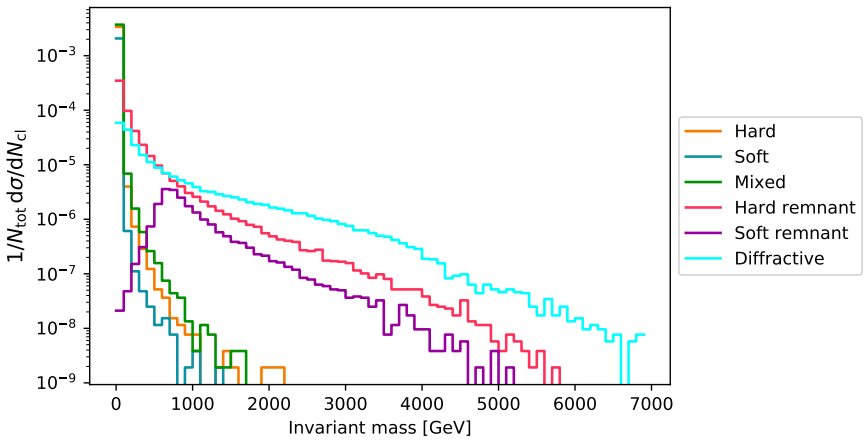

Figure 15: Invariant mass distribution of primary clusters normalized to the total number of primary clusters.

We observe that the diffractive and remnant primary cluster distributions have a long tails towards high invariant mass. As discussed in section 5.2 we suspect that this long tail is connected to the diffractive contribution in the last bin in the charged multiplicity. It is noteworthy that for a $\sqrt{s} = 7\,\text{TeV}$ collision the diffractive primary cluster distribution almost reaches 7 TeV, albeit heavily suppressed. However, events with a near 7 TeV primary cluster do not violate energy conservation since they also produce a small invariant mass primary cluster. Furthermore, due the high invariant mass of these clusters they will produce several iterations of cluster fission which will result in a large final state multiplicity. We believe that this large multiplicity is the contribution we observe in the last bin in figure 12.

6 Conclusion and Summary

In this work we have investigated the final state multiplicity by looking at hard and soft interactions in `Herwig7`'s MPI model. The results show how the charged multiplicity is related to the number of soft and hard interactions. From the heat map plot in figure 9 we observe that the number of hard and soft interactions are a driving factor for the charged multiplicity. This relation is expected due to the nature of MPI, however, the soft contribution is higher than expected. The results shown in figure 10 confirm that the hard interaction is the largest contributor to events with high charged multiplicity. While the soft interactions also contribute, they do so in the form of particles originating from mixed clusters. We confirm from figure 11 that the particles originating from mixed clusters are a product mainly due to color reconnection. We draw the overall conclusion that the charged multiplicity is linked to MPI and can mostly be accredited to the additional hard interactions for high multiplicities. This conclusion agrees with the logic that since the hard particles produce QCD radiation, they should contribute to higher charged multiplicity than the soft particles. Additionally, the color reconnection seems to be the driving force for the diversification of the final states through changing cluster constituents.
The labeling system was used to decompose observables into different contributions. The observable shown in figure 12 has a peak structure due to the soft particles which is most likely responsible for deviation from the data in the same region. Furthermore the deviation from the data grows after the point $N_{\text{ch}} = 50$ with the only noticeable contributions from particles labeled hard, mixed, hard remnant or diffractive. This large contribution from diffractive events in the last bin suggests that diffractive particles play a part in the deviation from data for that bin. A plausible explanation is that diffractive invariant masses are too large, therefore further investigation is needed.
For this purpose we produced the invariant mass distribution of primary clusters in figure 15. We did observe long tails for diffractive primary clusters and clusters with a remnant as a constituent. The long tail for diffractive events might be overestimated such that diffractive events contribute too much in the high charged multiplicity region.
For the high-$p_\perp$ part of the transverse momentum distribution in figure 13 the contribution

was almost exclusive to mixed and hard particles. This result is reasonable since the hard and mixed final state particles originate from a cluster where at least one constituent originates from a hard interaction. For the $p_\perp$ distribution shown in figure 14 we observed that the soft distribution extends further than $p_\perp^{\min}$. This result suggests that the cluster model used in `Herwig7` gives clusters additional transverse momentum such that the soft particles manage to have more transverse momentum than the threshold $p_\perp^{\min}$.

7 Outlook

The link between MPI and final state multiplicity could be used to get more efficient high multiplicity event generation. This could be useful since these events are quite suppressed such that it requires millions of events just to produce a few. The way to achieve this efficiency would be to exploit the way the number of hard and soft interactions are chosen in the simulation. In `Herwig7` the elements of the matrix from equation 2.3.14, are picked by a flat random distribution function from `ThePEG`. However, any distribution could be used and thus one could be constructed to only pick the events with a high number of soft and hard interactions. How this new distribution would affect the event generations and the observables could be a future endeavor. A concern is if diffractive events should be included, since they are important for some observables as seen in figure 12.
The labeling system introduced in this work is not only useful for model investigation such as shown in figure 14, but also for observable decomposition. This system could be used to investigate how different particles affect observables. The charged multiplicity observable in figure 12 has two interesting features: The soft peak in the low multiplicity region and the large contribution from the diffractive events in the last bin. These two phenomena could be further investigated with the labeling system. A future endeavor is to look for the reason why diffractive events contribute so much in the high multiplicity region. Before going deeper into the diffractive events it could be worth investigating invariant masses of diffractive clusters. For this purpose we did an investigation of primary cluster invariant mass which showed that the diffractive primary clusters did have a tail towards high invariant mass.
The diffractive final state particle gets contributions from events produced with zero hard interactions and zero soft interactions from the dummy matrix. However, an extended labeling system can be constructed for different diffractive processes as well which can exclude the dummy matrix contributions.
Furthermore the system could also be used as a tool for model tuning. An example is the cluster hadronization model, where the different labeled clusters could behave differently.
We would like to point out that most of the results produced in this work was thanks to the labeling system. The potential of this system could be further investigated in the future. The obvious next steps to take is to use this system to investigate for example restrictions to different interactions. In particular the large contribution of diffractive particles in the last bin in figure 12 suggest that a modification on diffractive cluster invariant masses

or diffractive events could be beneficial for the observable. The soft peak in the low multiplicity region is most likely the reason for the deviation from the data. Smoothing this soft peak could therefore help to make better simulations closer to the data. These examples above are but just a few ways the labeling system can be implemented. We could use the system to further understand the intricacies of models, for future development, improvements and to prepare event generation for future challenges.

Acknowledgments

I want to thank my supervisor Patrick Kirchgaeßer for making this bachelor project possible and for spending so much time guiding me. I am also grateful to my other supervisor Leif Lönnblad for his guidance, and for lending us his wisdom in event generation and particle physics. I want to thank the people from `Herwig7` for allowing me to join one of their meetings. I want to thank my fellow students and friends who gave me the strength and joy to carry on even through the most depressive and isolating moments of Covid-19. Last but definitely not the least i want to thank my mother for emotional support and for being a voice of reason.

References

[1]R. Bernhard, R. Field, R. Chierici, M. Cacciari, A. Moraes, M. Strikman, D. Treleani, T. C. Rogers, A. M. Stasto, A. Achilli, N. Moggi, L. Marti, F. Sikler, K. Krajczar, F. Ambroglini, P. Bartalini, L. Fano', F. Bechtel, W. Bell, A. Tricoli, A. Moraes, R. Grosso, J. F. Grosse-Oetringhaus, A. Carbone, D. Galli, U. Marconi, S. Perazzini, V. Vagnoni, F. Ferro, L. Frankfurt, H. Jung, R. McNulty, V. Lendermann, H. Kowalski, M. Gallinaro, L. Frankfurt, A. Solano, M. Arneodo, M. Campanelli, B. Blok, L. Frankfurt, J. Butterworth, T. Sjostrand, M. Bahr, S. Gieseke, M. H. Seymour, R. Corke, K. Werner, T. Pierog, S. Porteboeuf, H. Hoeth, P. Skands, D. D'Enterria, C. Marquet, A. Mischke, M. Estienne, and K. Reygers, *Proceedings of the first international workshop on multiple partonic interactions at the lhc (mpi08)*, 2010.

[2]T. Sjöstrand, S. Mrenna, and P. Skands, "Pythia 6.4 physics and manual", Journal of High Energy Physics **2006**, 026–026 (2006).

[3]Bähr, Manuel and Gieseke, Stefan and Gigg, Martyn A. and Grellscheid, David and Hamilton, Keith and Latunde-Dada, Oluseyi and Plätzer, Simon and Richardson, Peter and Seymour, Michael H. and Sherstnev, Alexander and et al., "Herwig++ physics and manual", The European Physical Journal C **58**, 639–707 (2008).

[4]A. Buckley, J. Butterworth, S. Gieseke, D. Grellscheid, S. Höche, H. Hoeth, F. Krauss, L. Lönnblad, E. Nurse, P. Richardson, and et al., "General-purpose event generators for lhc physics", Physics Reports **504**, 145–233 (2011).

[5]S. Gieseke, C. Röhr, and A. Siódmok, "Colour reconnections in herwig++", The European Physical Journal C **72**, 10.1140/epjc/s10052-012-2225-5 (2012).

[6]G. 't Hooft, "A Planar Diagram Theory for Strong Interactions", Nucl. Phys. B **72**, edited by J. C. Taylor, 461 (1974).

[7]D. Amati and G. Veneziano, "Preconfinement as a Property of Perturbative QCD", Phys. Lett. B **83**, 87–92 (1979).

[8]T. Sjöstrand, *Colour reconnection and its effects on precise measurements at the lhc*, 2013.

[9]T. Sjostrand and M. van Zijl, "A Multiple Interaction Model for the Event Structure in Hadron Collisions", Phys. Rev. D **36**, 2019 (1987).

[10]Bähr, Manuel, "Underlying Event Simulation in the Herwig++ Event Generator", PhD thesis (Karlsruhe U., 2008).

[11]M. V. Lokajicek, V. Kundrat, and J. Prochazka, *Elastic hadron scattering and optical theorem*, 2014.

[12]G. Aad, B. Abbott, J. Abdallah, A. A. Abdelalim, A. Abdesselam, O. Abdinov, B. Abi, M. Abolins, H. Abramowicz, H. Abreu, and et al., "Charged-particle multiplicities inppinteractions measured with the atlas detector at the lhc", New Journal of Physics **13**, 053033 (2011).